doi:10.1016/j.jmb.2007.07.019 J. Mol. Biol. (2007) 372, 847–854

JMB

Available online at www.sciencedirect.com

ScienceDirect

ELSEVIER

COMMUNICATION

Crystal Structure of the BIR1 Domain of XIAP in Two Crystal Forms

Su-Chang Lin, Yihua Huang, Yu-Chih Lo, Miao Lu and Hao Wu*

Department of Biochemistry Weill Medical College of Cornell University, New York NY 10021, USA

*Corresponding author

X-linked inhibitor of apoptosis (XIAP) is a potent negative regulator of apoptosis. It also plays a role in BMP signaling, TGF-β signaling, and copper homeostasis. Previous structural studies have shown that the baculoviral IAP repeat (BIR2 and BIR3) domains of XIAP interact with the IAP-binding-motifs (IBM) in several apoptosis proteins such as Smac and caspase-9 *via* the conserved IBM-binding groove. Here, we report the crystal structure in two crystal forms of the BIR1 domain of XIAP, which does not possess this IBM-binding groove and cannot interact with Smac or caspase-9. Instead, the BIR1 domain forms a conserved dimer through the region corresponding to the IBM-binding groove. Structural and sequence analyses suggest that this dimerization of BIR1 in XIAP may be conserved in other IAP family members such as cIAP1 and cIAP2 and may be important for the action of XIAP in TGF-β and BMP signaling and the action of cIAP1 and cIAP2 in TNF receptor signaling.

Keywords: crystal structure; XIAP; BIR1

Caspases are key executors of apoptosis, a cell elimination process crucial for the development and homeostasis of all multi-cellular organisms.[1] Inhibitors of apoptosis proteins (IAPs) are important negative regulators that guard the gate of cell death.[2–4] The most studied member of IAPs, X-linked IAP (XIAP), can inhibit caspases-3, -7 and -9 through its baculoviral IAP repeat (BIR) domains. Due to the potent caspase-inhibitory function of XIAP, it has been a therapeutic target for cancer treatment.[5,6]

Human XIAP has 497 amino acid residues, with three tandem BIR domains at the N-terminal region, followed by a RING domain that has E3 ubiquitin ligase activity at the C terminus. Each BIR domain contains a 70~80 amino acid zinc-binding motif. BIR2 (residues 163–234) with an upstream linker (residues 124–162) binds caspase-3 and −7.[7–9] While the linker directly blocks the active sites of caspase-3 and −7, the BIR2 domain enhances caspase inhibition through its interaction with the proteolytically generated N-terminal IAP-binding motif (IBM) of the small subunit of the caspases.[7–9] BIR3 (residues 256–349) selectively binds caspase-9 using a two-site binding mechanism.[10–12] One of the sites is the conserved IBM-interacting groove that interacts with the IBM sequence at the N-terminal end of processed caspase-9. The other site is the helix distal to BIR3, which packs against the dimer interface of caspase-9 to prevent the dimerization necessary for caspase activation.[11]

The IBM-interaction groove of BIR2 and BIR3 is also critical for Smac (also known as DIABLO) to relieve XIAP-mediated caspase inhibition to promote apoptosis.[13–16] The first residue of an IBM is always an Ala.[17] A single mutation of this residue in Smac (A1M) or a double mutation of the conserved acidic residue on the IBM-interaction groove of BIR2 and BIR3 (D214S and E314S) abolished XIAP–Smac interaction.[13–15]

XIAP has also been shown to bind to itself through its RING domain.[15] However, the oligomerization ability of the RING-deletion mutant of XIAP was only impaired but not completely abolished.[15] This suggests that the N-terminal BIR domains of XIAP

Present address: Y. Huang, Department of Biochemistry, University of Texas Southwestern Medical Center, Dallas, TX 75390, USA.

Abbreviations used: IAP, inhibitor of apoptosis protein; XIAP, X-linked IAP; IBM, IAP-binding motif; BIR, baculoviral IAP repeat.

E-mail address of the corresponding author: haowu@med.cornell.edu

Table 1. Crystallographic statistics

	BIR1	BIR1
Constructs	Residues 20–99	Residues 20–99
Structure determination	SAD	MR
Molecules/a.u.	1	4
Data collection		
Beamlines	X4A of NSLS	X4A of NSLS
Space group	*I*222	$P2_1$
Cell dimensions		
a, *b*, *c* (Å), β(°)	34.9, 73.0, 81.7	35.6, 73.0, 68.9, 95.7
Resolution (Å)	30–1.8	30–2.5
R_{sym} (%)	6.0 (22.8)[a]	4.3 (10.4)
$I/\sigma I$	22.9 (4.9)	33.1 (10.2)
Completeness (%)	92.3 (61.5)	98.1 (75.5)
Redundancy	6.5 (3.7)	3.5 (2.8)
Refinement		
Resolution (Å)	30–1.8	30–2.5
No. reflections	9122	12,283
R_{work}/R_{free} (%)	19.8/21.4	19.6/25.3
No. atoms		
Protein	618	2508
Water and ion	91	87
Average *B*-factors (Å^2)		
Protein	28.1	47.6
Water and ion	39.3	41.2
RMSDs		
Bond lengths (Å)/ angles(°)	0.006/1.17	0.010/1.37
Ramachandran plot (%)		
Most favored/allowed	90.9/9.1	85.1/14.9

BIR1 protein was expressed by the pGEX-4T-3 vector with an insert of human XIAP cDNA encoding the first BIR domain (BIR1, residue 1–123) and purified by affinity chromatography. The GST tag was removed by thrombin protease digestion and the BIR protein was further purified by gel filtration. To obtain better crystals, the BIR1 protein was subjected to limited proteolysis with subtilisin (a 1:500 molar ratio, 4 °C for 2 h). A fragment with residues 20–99 was identified by N-terminal protein sequencing and mass spectroscopy analyses. The cDNA encoding this fragment was further sub-cloned into the pGEX4T-3 vector. The expressed protein was crystallized under two conditions. Crystals with the space group $P2_1$ were obtained with a reservoir composed of 15% (v/v) ethanol, 100 mM sodium citrate (pH 5.5) and 200 mM Li_2SO_4. Crystals with the space group *I*222 were gained under a condition with 1.5 M NaCl, 10% (v/v) methanol, and 100 mM Hepes (pH 7.5). The structure of *I*222 crystals was solved by SAD (single wavelength anomalous diffraction). Data were collected at a zinc absorption peak for phase determination at the Brookhaven NSLS. The zinc site was found using the Shake & Bake program and refined using SOLVE/RESOLVE. The model was built using the Arp/warp program and refined using the CNS package. The structure of the $P2_1$ crystals was solved by the molecular replacement (MR) method, as implemented in the CNS package, using the structure of *I*222 crystals as a starting model.

[a] Highest resolution shell is shown in parenthesis.

could also oligomerize. Besides caspases, Smac and itself, XIAP could bind to several other partners, including HtrA2/Omi, TAB1, the bone morphogenetic protein receptor, TGF-β type I receptor, MURR1, GdH, Nsp4, 3HB, and Slim1.[15,18–21] Most of the binding sites for these partners were mapped to the BIR2, BIR3, and RING domains[13–15,18,19,22] The BIR1 domain has no ascribed function.

Sequence alignments of BIR1 domains show that BIR1 is conserved across species, suggesting that it may be important for some aspect of XIAP function. Here, we report two crystal structures of the BIR1 domain of XIAP, at 1.8 Å and 2.5 Å, respectively. The structures identified critical changes in BIR1 that are responsible for the lack of ability to interact with IBMs. They also revealed a conserved BIR1 dimer that may be important for the signaling functions of XIAP and implicated BIR1 as another dimerization domain for multiple IAP family members.

The BIR1 structure in two crystal forms

The BIR1 structures were determined at 1.8 Å and 2.5 Å resolutions in space groups *I*222 and $P2_1$, respectively (Table 1). There are four independent BIR1 molecules in the crystallographic asymmetric unit of the $P2_1$ space group and one BIR1 molecule in the *I*222 space group. The crystallization conditions of the two crystals differ in pH, salt and alcohol concentrations. However, the BIR1 domain structures in both crystals are very similar, with root-mean-square deviations (RMSDs) ranging from 0.47 Å to 0.60 Å.

The BIR1 structure (residues 22–99) consists of a three-stranded β-sheet, surrounded by four helices, and a zinc atom chelated by three Cys and one His residue (Cys63, Cys66, His83 and Cys90) (Figure 1(a)). The BIR1 structure resembles the core structures of BIR2 (Ala159–Arg233) and BIR3 (Ser261–Glu332), both with an RMSD value of 0.97 Å (Figure 1(b)).

Differences in the IBM-binding groove

In BIR1, residues corresponding to those that interact with the first IBM residue in BIR2 and BIR3 are Val70, Asp71 (backbone O atom), Trp73, Asp77, Arg82, and Val86 (Figure 1(a)). Val70 and Trp73 form the bottom of the IBM-interaction groove. Asp77 is a conserved acidic residue that plays a critical role in interacting with the amino group at the first IBM residue. The BIR1 residues Arg82 and Val86 are different in BIR2 and BIR3.

To elucidate the defect of BIR1 in IBM-binding, we compared the structures of the IBM-binding region of the three BIR domains of XIAP. The side-chain of Arg82 is about 1.7 Å longer than the corresponding residues Glu219 and Gln319 in BIR2 and BIR3, respectively. It protrudes into the IBM-interaction groove, which causes steric hindrance in the binding pocket for the first IBM residue (Figure 1(c)). Val86 is shorter than His223 and W323 in BIR2 and BIR3, respectively. The replacement of Val86 for His223/W323 will reduce the van der Waals interactions between BIR1 and an IBM. Therefore, according to the BIR1 crystal structure, Arg82 and Val86 interfere with the BIR1–caspase and BIR1–Smac interactions (Figure 1(c)–(f)).

In agreement with previous reports, E219R/H223V double mutations weakened XIAP-mediated caspase-3 and -7 inhibition and abolished the BIR2–Smac interaction.[23] Similar mutations on cIAP1 (E239R and H243V in BIR2 and E325R and W329V in BIR3) also ablated the ability of the BIR domains to associate with caspase-7.[24]

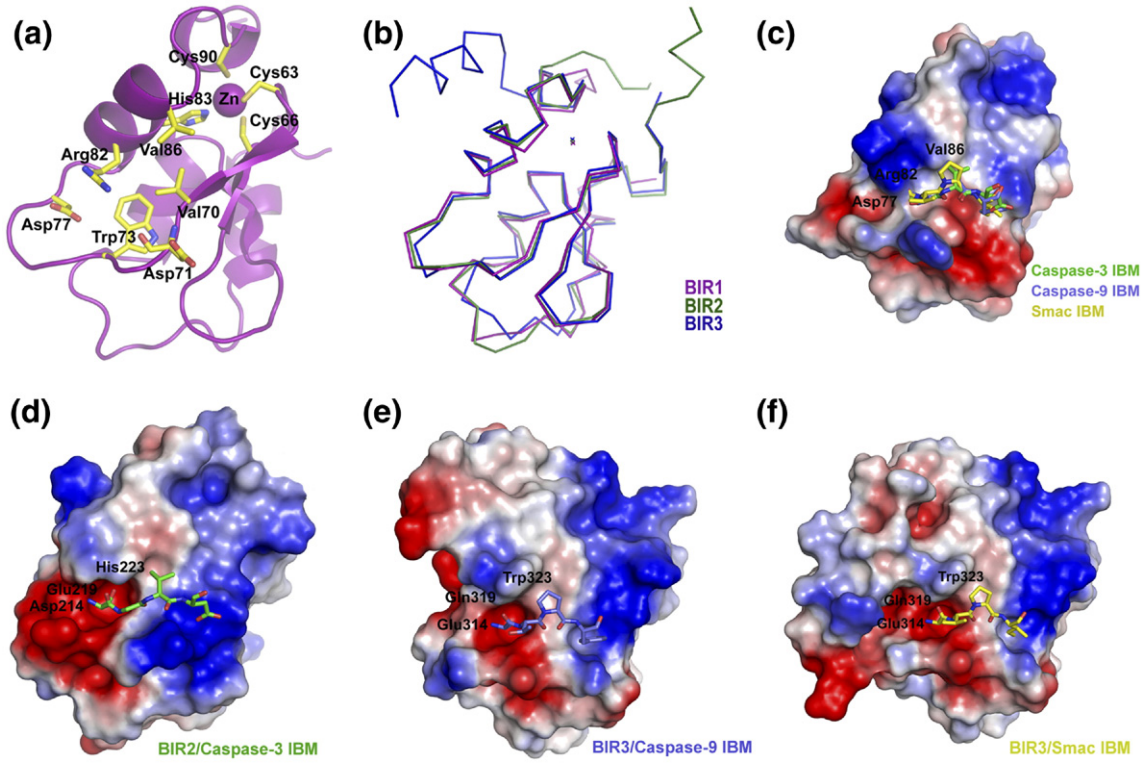

Figure 1. The structure and IBM-binding groove of the BIR domains of XIAP. (a) A ribbon diagram of BIR1. The important residues for BIR–IBM interaction are labeled. The residues chelating the zinc ion are also shown. (b) Superposition of the C^{α} traces of the three BIR domains of XIAP. (c) Electrostatic surface representation of BIR1. Three IBM fragments from the superimposed BIR–IBM complexes (in (d)–(f)) are shown in stick format. The first residue of all IBMs is buried in the electrostatic surface of Arg82, which indicates a steric hindrance in the binding of the first IBM residue. (d)–(f) Electrostatic surface representation of the BIR–IBM complexes from the BIR2–caspase-3 complex ((d); PDB ID, 1I3O), BIR3–caspase-9 complex ((e); PDB ID, 1NW9), and BIR3–Smac complex ((f); PDB ID, 1G73). For clarity, only part of the BIR2 domain is shown in (e).

BIR1 forms a conserved dimer in both crystal forms

Four BIR1 molecules form two very similar dimers in the asymmetric unit of the $P2_1$ crystal (Figure 2(a)). These two BIR1 dimers superimpose to an RMSD of 0.6 Å. The similar BIR1 dimer in the $P2_1$ crystal was also found in the *I*222 crystal by inspecting the crystal packing, although there is a monomer per asymmetric unit (Figure 2(a)). The BIR1 dimer architectures in the two crystal forms are similar but show some differences, with RMSD values ranging from 1.96 Å to 2.30 Å. While the BIR1 dimers in the $P2_1$ crystal are pseudo-symmetric, the BIR1 dimer in the *I*222 crystal is perfectly symmetric.

The symmetric BIR1 dimer interface consists of 16 hydrogen bonds and two van der Waals contact regions (Figure 2(b) and (e)). The total buried surface area is about 1300 $Å^2$. Hydrogen bonds play an essential role in dimer formation. There are four ionic hydrogen bonds between two Arg72–Asp77 and two Asp71—Arg82 pairs. The side-chains of each Arg72 and each Arg62 also donate a hydrogen bond to the main-chain O atom of Arg72 and Lys85 in the dimer partner, respectively. Additional hydrogen bonds are formed between two Thr60–Lys85 and two Asp71–Lys85 pairs. In addition to the hydrogen-bonding network, van der Waals contacts also appear to be important in stabilizing the dimer formation. One van der Waals interaction area is located at Ala68, Ala69 and Val86. The other one is generated by the multiple contacts among residues.

Most of the inter-molecular interactions seen in the *I*222 symmetric BIR1 dimer are conserved in the $P2_1$ dimers, although the latter are less extensive with about 1000 $Å^2$ of buried surface area and consist of 14 hydrogen bonds and the similar two patches of van der Waals interactions (Figure 2(c) and (f)). Only few changes in the hydrogen bonding and van der Waals contacts are observed on the dimerization interface. Each Arg62 donates a hydrogen bond to the main-chain O atom of Val86 instead of Lys85. Arg72 forms another two hydrogen bonds with Gln74 and Arg82, but only two hydrogen bonds form between Thr60–Lys85 and Asp71–Lys85. Val86 contacts a smaller hydrophobic patch formed by Arg62 and Ala69 of the other molecule.

The differences in the dimer architectures appear to be brought about by the different packing environments in the two crystals (Figure 2(d)). In the *I*222 crystal, there are no other packing interactions near the dimerization interface, making this the likely physiological form of the dimer. In contrast, in the $P2_1$ crystal, an exposed Tyr side-chain

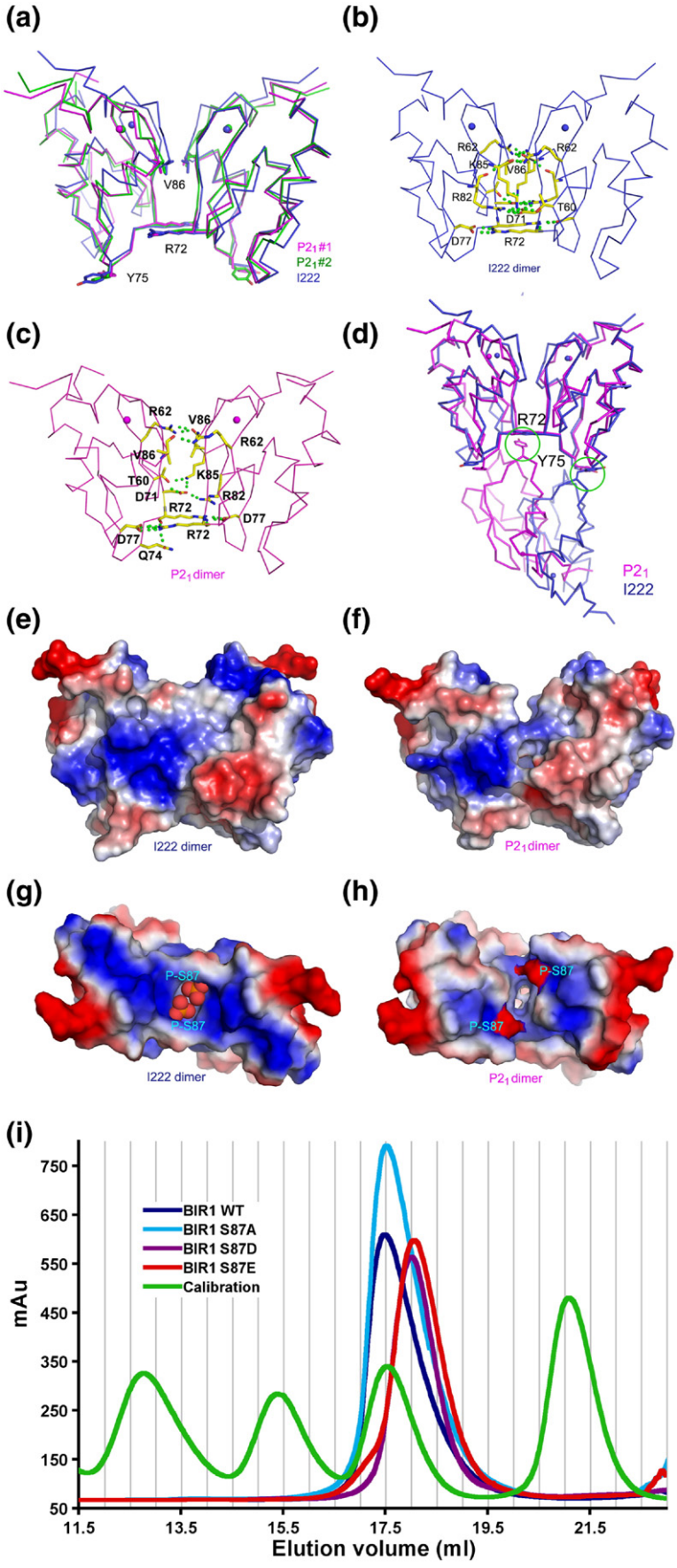

Figure 2. Structure of the BIR1 dimer. (a) Superposition of the C^{α} traces of the three BIR1 dimers in the two crystal forms. (b) The inter-molecular interactions in the symmetric BIR1 dimer of the *I*222 crystal. (c) The inter-molecular interactions in the asymmetric BIR1 dimer of the $P2_1$ crystal. (d) The different packing interactions for the BIR1 dimers in the $P2_1$ crystal and the *I*222 crystal. The C^{α} traces of the BIR1 dimers in the two crystal forms were superimposed and a neighboring BIR1 in the crystal is shown. The interactions between Tyr75 and neighboring dimers are highlighted with green circles. (e)–(f) Electrostatic surface representations of the BIR1 dimer in the *I*222 crystal (e) and the $P2_1$ crystal (f). (g)–(h) Electrostatic surface representations, shown by rotating the models in (e) and (f), respectively, by 90° along the horizontal axis. The phosphoserine was manually docked on S87 and shown as sphere and red surfaces in (g) and (h), respectively. (i) Superimposed gel filtration profiles of wild-type, S87A, S87D and S87E mutants of BIR1. The calibration markers, from left to right, are of molecular masses 158 kDa, 44 kDa, 17 kDa and 1.35 kDa, respectively.

from a neighboring BIR1 molecule inserts into the dimerization interface (Figure 2(d)). This is true for both dimers in this crystal form, making the dimerization somewhat asymmetric and less extensive in comparison with the *I*222 dimer. Although there are some differences between the dimers in the two crystal forms, the apparent similar dimers suggest that BIR1 is one of the XIAP dimerization domains.

Interestingly, the same BIR1 dimer is also observed in the crystal structure of the BIR1–TAB1 complex and BIR1 was shown to have a tendency to dimerize in solution.[25] TAB1 is an upstream adapter for the activation of the kinase TAK1, which in turn couples XIAP to the NF-κB pathway. Structure-based mutagenesis showed that disruption of BIR1 dimerization abolishes XIAP-mediated NF-κB activation.

A common interaction interface of BIR domains

It is interesting that the IBM-interacting residues of BIR2 and BIR3 and the self-dimerization residues of BIR1 are both located in a region containing β3 and α3, which is tightly restrained by the bound zinc. The IBM-interacting residues and self-dimerization residues are significantly overlapped (Figure 3), suggesting an evolutionarily conserved role of this region in protein–protein interactions.

The different chemical properties of residues in this zinc-restrained region determine its role in either dimerization or IBM interaction. In BIR2 and BIR3, the critical conserved acidic residue (Asp214 and Glu314) interacts with the N-terminal amino group of the IBM (Figure 1(d)–(f)). In BIR1, the corresponding acidic residue (Asp77) interacts with the side-chain guanidinium group of Arg72, which may mimic the N-terminal amino group of the IBM (Figure 2(b) and (c)). Residues Glu219 and Gln319 of BIR2 and BIR3, respectively, interact with the N-terminal residue of the IBM. The corresponding residue, Arg82 in BIR1, forms multiple contacts with Arg72 and other residues as described above. Furthermore, His223 and W323 of BIR2 and BIR3, respectively, form multiple contacts with the second and third IBM residues. The corresponding residue, Val86 in BIR1, interacts with several residues of the dimeric partner.

To see if BIR2 and BIR3 could form a dimer as BIR1, we superimposed BIR2 and BIR3 structure on the BIR1 dimer. The superpositions show that a steric hindrance by His223/Phe224 and Trp323/Tyr324, respectively, may prevent dimer formation of BIR2 and BIR3. A previous study has shown that either the wild-type or the D214S/E314S double mutant of the RING-deleted XIAP retain similar partial ability in dimerization.[15] In addition, all NMR analyses have shown that both BIR2 and BIR3 domains, alone or bound with an IBM, are monomers in solution.[26–28] These data support that BIR1, not BIR2 and BIR3, functions as an XIAP dimerization domain.

A conserved sequence pattern for self-dimerization

To see if other IAPs may carry a similar sequence pattern as BIR1 for self-dimerization, we performed a sequence-homology search using the PATTINPROT program against the protein sequence database.[29] The result shows that a conserved sequence pattern of [K/R/Q]-C-X(2)-C-X(4)-D-[R/N]-W-X(3)-D-X(4)-[K/R]-H-X-[K/R/Q]-[V/I/L]-X(3)-C (7 out of the 11 dimerization residues underlined) could be found in the BIR1 domains of the XIAP analogues, cIAP1 and cIAP2. This suggests that the BIR1 domain of these IAPs may also mediate dimerization (Figure 3).

BIR1-mediated dimerization of cIAP2 is supported by experimental data. Recently, the BIR1 domain of cIAP2 was shown to be necessary for dimerization or oligomerization of the cIAP2–MALT1 fusion protein in NF-κB activation in MALT lymphomas.[30] Both cIAP1 and cIAP2 are constitutively associated with TRAF1 and TRAF2, two proteins involved in TNF signaling.[31] This interaction has been mapped to the BIR1 domain, in the α1 and the α2 region opposite of the putative BIR1 dimerization interface.[32,33] Mutants of the cIAP2–MALT1 fusion protein that cannot interact with TRAF2 still dimerize or oligo-

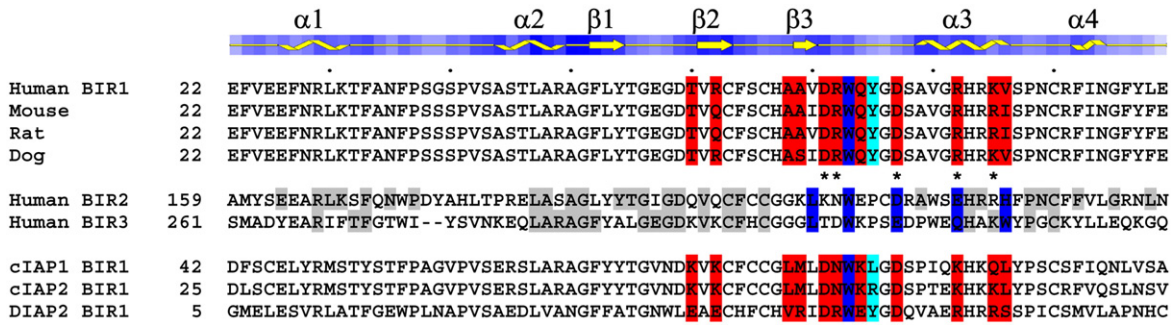

Figure 3. Structure-based sequence alignment. Secondary structures of XIAP BIR1 are labeled. The top four rows are the BIR1 of XIAP from different species. Residues at the dimer interface are highlighted in red, and residues that form the hydrogen bond network at the interface are labeled with an asterisk (*). Residues of BIR2 and BIR3 of XIAP identical to BIR1 are highlighted in grey. Residues that form the IBM-binding groove are highlighted in blue. The last three rows are the BIR1 sequences of several different IAPs.

merize,[33] suggesting that BIR1-mediated cIAP2 dimerization is probably through the region with the conserved sequence pattern reported here.

A similar sequence pattern for BIR1 self-dimerization could also be found in the BIR1 domain of a *Drosophila* IAP, DIAP2. Although there is no available experimental evidence, we predict that this BIR1 domain also mediates dimerization in DIAP2.

Phosphorylation of S87 may modulate BIR1 dimerization

Interestingly, S87 of XIAP, a residue near the BIR1 dimerization interface, is the target of phosphorylation by Akt kinases.[34] It was shown that Akt interacts with and phosphorylates XIAP both *in vitro* and *in vivo*. This phosphorylation prevents XIAP self-ubiquitination and degradation and is important for Akt-mediated cell survival. Based on the dimer structures reported here, we modeled phosphoserine to S87 in both the symmetric and the asymmetric dimers (Figure 2(g) and (h)). Both S87-phosphorylated BIR1 models show no steric hindrances by the phosphorylation. However, given the location of S87 near the dimerization interface, it is possible that S87 phosphorylation would generate sufficient charge repulsion to disrupt BIR1 dimerization.

To test the hypothesis on the role of S87 phosphorylation in BIR1 dimerization, we generated the phospho-mimic mutations S87D and S87E and an Ala mutation S87A. Gel filtration chromatography showed that wild-type BIR1 and its S87A mutant both eluted at a position near the 17 kDa calibration marker (Figure 2(i)). Because the calculated molecular mass of BIR1 is 12.4 kDa, this elution position suggested that both the wild-type and S87A mutant of BIR1 are in equilibrium between dimer and monomer in solution. In contrast, the phospho-mimic mutants S87D and S87E of BIR1 both eluted approximately 0.5 ml later, consistent with disruption of dimerization in these mutants (Figure 2(i)). Therefore, inhibition of XIAP self-ubiquitination by S87 phosphorylation may be due to inhibition of BIR1 dimerization.

Other potential interaction interface

It is unusual to have large hydrophobic residues extending outward from the protein surface. Noteworthy, a turn in the middle of the zinc-restrained region, containing residues Tyr75 and Gly76 in BIR1 of XIAP, protrudes into the solvent and could play a role in protein–protein interactions (Figure 2(a)). In $P2_1$ crystals, two Tyr75 side-chains make multiple contacts with Asp59, Arg72, and Gln74 on other BIR1 molecules in the crystal lattice (Figure 2(d)). These interactions are responsible for the differences in the BIR1 dimer architectures in the two crystal forms. Tyr75 in the *I*222 crystal also make extensive interactions, with Gly39, Ser40, and Pro41 of the symmetrical molecule. The interactions bury about 135 Å^2 (72%) and 120 Å^2 (53%) of the solvent accessible area of Tyr75 in the $P2_1$ crystal and the *I*222 crystal, respectively.

The lack of a side-chain in Gly76 allows flexible rotations of the Tyr75 side-chain. In fact, the side-chain of Tyr75 rotates about 116 degrees along the C^{α}–C^{β} axis when the two crystal structures are superimposed (Figure 2(a)). The flexible side-chain rotations of Tyr75 might allow an induced-fit during any potential protein interactions. In fact, in one BIR1 molecule in the $P2_1$ crystal, the side-chain of Tyr75 has no lattice contact and is disordered. Collectively, these observations suggest that Tyr75 likely defines another region of protein interaction interface in BIR1.

Summary

In conclusion, the loop with both ends tightly restrained by the bound zinc in the BIR domain is an evolutionally conserved interface that plays an important role in BIR–protein interaction. In addition to the known BIR–Smac and BIR–caspase interaction as an IBM-binding groove, here we report that it is also a dimerization motif in BIR1.

A conserved sequence pattern for BIR1 dimerization can be found in the BIR1 domains of XIAP, cIAP1, cIAP2 and DIAP2. Despite many reports discussing the interactions between BIR2/BIR3 and IBM-containing proteins, little is known about the function of the BIR1 domain. Recently, dimerization of BIR1 has been proven to be critical for cIAP2–MALT1 fusion protein-mediated NF-κB activation and contributing to MALT lymphomas.[33] In addition, BIR1 can bind TRAF1 and TRAF2, and BIR1–TRAF2 interaction is important for cIAP1 and cIAP2 in TRAF2-mediated regulation of NF-κB in TNF receptor signaling.[32,33] Besides, DIAP2 is required for the immune deficiency (Imd) signaling pathway, which is similar to the TNFR1 signaling cascade,[35] protecting flies from Gram-negative bacterial infection.[36,37] For XIAP, its signaling function may be in the coupling to the TAK1 kinase pathway for NF-κB activation.[19] All these signaling pathways may require the BIR1 dimerization by the conserved interaction observed here.

Acknowledgements

This work was supported by the National Institutes of Health (RO1 AI045937 to H.W.). S.-C.L. and Y.-C.L. are postdoctoral fellows of the Cancer Research Institute and M. L. is a postdoctoral fellow of the American Heart Association.

References

1. Danial, N. N. & Korsmeyer, S. J. (2004). Cell death: critical control points. *Cell*, **116**, 205–219.
2. Deveraux, Q. L., Takahashi, R., Salvesen, G. S. & Reed,

J. C. (1997). X-linked IAP is a direct inhibitor of cell-death proteases. *Nature*, **388**, 300–304.
3. Miller, L. K. (1999). An exegesis of IAPs: salvation and surprises from BIR motifs. *Trends Cell Biol.* **9**, 323–328.
4. Deveraux, Q. L. & Reed, J. C. (1999). IAP family proteins-suppressors of apoptosis. *Genes Dev.* **13**, 239–252.
5. Schimmer, A. D., Dalili, S., Batey, R. A. & Riedl, S. J. (2005). Targeting XIAP for the treatment of malignancy. *Cell Death Differ.* **13**, 179–188.
6. Fischer, U. & Schulze-Osthoff, K. (2005). New approaches and therapeutics targeting spoptosis in disease. *Pharmacol. Rev.* **57**, 187–215.
7. Huang, Y., Park, Y. C., Rich, R. L., Segal, D., Myszka, D. G. & Wu, H. (2001). Structural basis of caspase inhibition by XIAP: differential roles of the linker versus the BIR domain. *Cell*, **104**, 781–790.
8. Chai, J., Shiozaki, E., Srinivasula, S. M., Wu, Q., Dataa, P., Alnemri, E. S. & Shi, Y. (2001). Structural basis of caspase-7 inhibition by XIAP. *Cell*, **104**, 769–780.
9. Riedl, S. J., Renatus, M., Schwarzenbacher, R., Zhou, Q., Sun, C., Fesik, S. W. *et al.* (2001). Structural basis for the inhibition of caspase-3 by XIAP. *Cell*, **104**, 791–800.
10. Shiozaki, E. N., Chai, J., Rigotti, D. J., Riedl, S. J., Li, P., Srinivasula, S. M. *et al.* (2003). Mechanism of XIAP-mediated inhibition of caspase-9. *Mol. Cell*, **11**, 519–527.
11. Eckelman, B. P., Salvesen, G. S. & Scott, F. L. (2006). Human inhibitor of apoptosis proteins: why XIAP is the black sheep of the family. *EMBO Rep.* **7**, 988–994.
12. Fuentes-Prior, P. & Salvesen, G. S. (2004). The protein structures that shape caspase activity, specificity, activation and inhibition. *Biochem. J.* **384**, 201–232.
13. Chai, J., Du, C., Wu, J.-W., Kyin, S., Wang, X. & Shi, Y. (2000). Structural and biochemical basis of apoptotic activation by Smac/DIABLO. *Nature*, **406**, 855–862.
14. Wu, G., Chai, J., Suber, T. L., Wu, J.-W., Du, C., Wang, X. & Shi, Y. (2000). Structural basis of IAP recognition by Smac/DIABLO. *Nature*, **408**, 1008–1012.
15. Silke, J., Hawkins, C. J., Ekert, P. G., Chew, J., Day, C. L., Pakusch, M. *et al.* (2002). The anti-apoptotic activity of XIAP is retained upon mutation of both the caspase 3- and caspase 9-interacting sites. *J. Cell Biol.* **157**, 115–124.
16. Huang, Y., Rich, R. L., Myszka, D. G. & Wu, H. (2003). Requirement of both the second and third BIR domains for the relief of X-linked inhibitor of apoptosis protein (XIAP)-mediated caspase inhibition by Smac. *J. Biol. Chem.* **278**, 49517–49522.
17. Franklin, M. C., Kadkhodayan, S., Ackerly, H., Alexandru, D., Distefano, M. D., Elliott, L. O. *et al.* (2003). Structure and function analysis of peptide antagonists of melanoma inhibitor of apoptosis (ML-IAP). *Biochemistry*, **42**, 8223–8231.
18. Verhagen, A. M., Kratina, T. K., Hawkins, C. J., Silke, J., Ekert, P. G. & Vaux, D. L. (2006). Identification of mammalian mitochondrial proteins that interact with IAPs via N-terminal IAP binding motifs. *Cell Death Differ.* **14**, 348–357.
19. Yamaguchi, K., Nagai, S., Ninomiya-Tsuji, J., Nishita, M., Tamai, K., Irie, K. *et al.* (1999). XIAP, a cellular member of the inhibitor of apoptosis protein family, links the receptors to TAB1-TAK1 in the BMP signaling pathway. *EMBO J.* **18**, 179–187.
20. Burstein, E., Ganesh, L., Dick, R. D., van De Sluis, B., Wilkinson, J. C., Klomp, L. W. *et al.* (2004). A novel role for XIAP in copper homeostasis through regulation of MURR1. *EMBO J.* **23**, 244–254.
21. Reffey, S. B., Wurthner, J. U., Parks, W. T., Roberts, A. B. & Duckett, C. S. (2001). X-linked inhibitor of apoptosis protein functions as a cofactor in transforming growth factor-beta signaling. *J. Biol. Chem.* **276**, 26542–26549.
22. Suzuki, Y., Imai, Y., Nakayama, H., Takahashi, K., Takio, K. & Takahashi, R. (2001). A serine protease, HtrA2, is released from the mitochondria and interacts with XIAP, inducing cell death. *Mol. Cell*, **8**, 613–621.
23. Scott, F. L., Denault, J. B., Riedl, S. J., Shin, H., Renatus, M. & Salvesen, G. S. (2005). XIAP inhibits caspase-3 and -7 using two binding sites: evolutionarily conserved mechanism of IAPs. *EMBO J.* **24**, 645–655.
24. Eckelman, B. P. & Salvesen, G. S. (2006). The human anti-apoptotic proteins cIAP1 and cIAP2 bind but do not inhibit caspases. *J. Biol. Chem.* **281**, 3254–3260.
25. Lu, M., Lin, S. C., Huang, Y., Kang, Y. J., Rich, R. L., Lo, Y. C. *et al.* (2007). XIAP induces NF-kappaB activation via the BIR1/TAB1 interaction and BIR1 dimerization. *Mol. Cell*, **26**, 689–702.
26. Sun, C., Cai, M., Gunasekera, A. H., Meadows, R. P., Wang, H., Chen, J. *et al.* (1999). NMR structure and mutagenesis of the inhibitor-of-apoptosis protein XIAP. *Nature*, **401**, 818–822.
27. Sun, C., Cai, M., Meadows, R. P., Xu, N., Gunasekera, A. H., Herrmann, J. *et al.* (2000). NMR structure and mutagenesis of the third Bir domain of the inhibitor of apoptosis protein XIAP. *J. Biol. Chem.* **275**, 33777–33781.
28. Liu, Z., Sun, C., Olejniczak, E. T., Meadows, R. P., Betz, S. F., Oost, T. *et al.* (2000). Structural basis for binding of Smac/DIABLO to the XIAP BIR3 domain. *Nature*, **408**, 1004–1008.
29. Combet, C., Blanchet, C., Geourjon, C. & Deleage, G. (2000). NPS@: network protein sequence analysis. *Trends Biochem. Sci.* **25**, 147–150.
30. Zhou, H., Du, M.-Q. & Dixit, V. M. (2005). Constitutive NF-[kappa]B activation by the t(11;18)(q21;q21) product in MALT lymphoma is linked to deregulated ubiquitin ligase activity. *Cancer Cell*, **7**, 425–431.
31. Rothe, M., Pan, M. G., Henzel, W. J., Ayres, T. M. & Goeddel, D. V. (1995). The TNFR2-TRAF signaling complex contains two novel proteins related to baculoviral inhibitor of apoptosis proteins. *Cell*, **83**, 1243–1252.
32. Samuel, T., Welsh, K., Lober, T., Togo, S. H., Zapata, J. M. & Reed, J. C. (2006). Distinct BIR domains of cIAP1 mediate binding to and ubiquitination of tumor necrosis factor receptor-associated factor 2 and second mitochondrial activator of caspases. *J. Biol. Chem.* **281**, 1080–1090.
33. Varfolomeev, E., Wayson, S. M., Dixit, V. M., Fairbrother, W. J. & Vucic, D. (2006). The inhibitor of apoptosis protein fusion c-IAP2{middle dot}MALT1 stimulates NF-{kappa}B activation independently of TRAF1 AND TRAF2. *J. Biol. Chem.* **281**, 29022–29029.
34. Dan, H. C., Sun, M., Kaneko, S., Feldman, R. I., Nicosia, S. V., Wang, H.-G. *et al.* (2004). Akt phosphorylation and stabilization of X-linked inhibitor of apoptosis protein (XIAP). *J. Biol. Chem.* **279**, 5405–5412.
35. Tanji, T. & Ip, Y. T. (2005). Regulators of the Toll and Imd pathways in the *Drosophila* innate immune response. *Trends Immunol.* **26**, 193–198.
36. Leulier, F., Lhocine, N., Lemaitre, B. & Meier, P. (2006).

The *Drosophila* inhibitor of apoptosis protein DIAP2 functions in innate immunity and is essential to resist Gram-negative bacterial infection. *Mol. Cell. Biol.* **26**, 7821–7831.
37. Huh, J. R., Foe, I., Muro, I., Chen, C. H., Seol, J. H., Yoo, S. J. *et al.* (2007). The *Drosophila* inhibitor of apoptosis (IAP) DIAP2 is dispensable for cell survival, required for the innate immune response to Gram-negative bacterial Iinfection, and can be negatively regulated by the Reaper/Hid/Grim family of IAP-binding apoptosis inducers. *J. Biol. Chem.* **282**, 2056–2068.

Edited by I. Wilson

(Received 9 April 2007; received in revised form 25 June 2007; accepted 10 July 2007)
Available online 21 July 2007